Effect of different electric fields on temperature rise, energy efficiency ratio, and solids content during electro-osmotic dewatering of tofu residue (okara)

報　文

Effect of different electric fields on temperature rise, energy efficiency ratio, and solids content during electro-osmotic dewatering of tofu residue (okara)

Fa-De Li,[a,b,c] Xiuqu Li,[b] Itaru Sotome,[b] and Seiichiro Isobe[b, §]

[a] College of Mechanical and Electronic Engineering, Shandong Agricultural University, Taian 271018,
Shandong Province, P. R. China
[b] National Food Research Institute, Kannondai, Tsukuba, Ibaraki 305-8642, Japan
[c] UNU-KIRIN Fellow

Abstract

A large amount of tofu residue (okara) is created by the traditional soybean food (e.g. tofu and soymilk) manufacturing industry every year in Japan. For wide utilization of okara, a high-efficiency dewatering technique is essential. The present study investigated the feasibility of electro-osmotic dewatering (EOD) of okara under pressure (70 kPa) with a horizontal electric field (both electrodes were titanium sieves, 14 mesh) that was characterized by a DC, an AC (with square waveform), and a duty ratio (DR; with rectangular waveform) voltage (20 V RMS). The results confirmed that the temperature rise could not be ignored under any kind of electric field. It was found that the water within the sample moved towards both electrodes simultaneously, especially in the initial EOD period. The mass of drainage increased with an increase in DC voltage. However, the frequency and the DR had no significant effect on the total drainage. The energy efficiency ratio, defined as the ratio of the energy consumed for evaporating the excess removed water to the energy input to the electric field for EOD, exceeded one within the initial period; however, it decreased quickly and was lower than one with dewatering. Although the Joule heat losses resulted in a decreased energy efficiency ratio during EOD, the temperature rise had the positive effects of pasteurization and deactivation on some antinutritional factors, especially trysin inhibitor. The solids content of the drainage removed by the EOD course was lower than that removed by mere pressure; it decreased with an increase in DC voltage, but increased with an increase in frequency. However, the DR of the voltage had no significant effect on the solids content under the experiment conditions.

The results of this study should be helpful not only to okara dewatering, but also to the reuse of other high moisture content byproducts in the food industry.

Keywords: Tofu residue, Okara, Electro-osmotic dewatering, Energy efficiency ratio, Solids content.

Introduction

Tofu residue, usually called okara, is the fiber, protein, and starch left over when soy milk has been extracted from ground soaked soybeans. Traditional soybean food (e.g. soymilk, tofu, and processed tofu) is highly appreciated throughout the world, especially in Asia. For example, more

---

than 4×10^6 tons of soybeans in China[1] and 1×10^6 tons in Japan are used for processing traditional soy food every year. According to Khare et al.,[2] 1.1 kg of fresh okara is produced from every kilogram of soybeans processed for soymilk or tofu. In Japan, the mass ratio of okara to dry soybean is about 1.4 on a commercial scale.

Typically, okara has 75% to 80% moisture content on a wet basis and 60% fiber, 29% protein, and 11% fat on a dry basis.[3] Although these components are water-insoluble, okara should not be regarded as a waste product; it can be widely utilized as an ingredient of food or as animal feed.[4,5] In recent years, it has been used as culture medium for producing fungal chitosan,[6] *Ganoderma lucidum*,[7] xylanase,[8] oil components,[9] and some biodegradable materials (e.g. seedling culture pots).[10,11] However, because of its high moisture content, it spoils easily in natural conditions. For large-scale utilization, it should be preserved under appropriate conditions. One economical and feasible method of preservation is to reduce the moisture content of okara soon after production.

Some drying methods for okara were summarized by O'-Toole.[4] In addition, Taruna et al. used a continuously vortex-like moving bed for drying okara and found that the specific heat consumption was three to four times higher than that for free water.[3] Wachiraphansakul et al.[12] reported that the minimum specific energy consumption for drying okara was 3.69 MJ kg^{-1} for evaporating water under the optimum operation parameters. Li et al.[13,14] reported that the electrohydrodynamic technique not only promotes the drying rate, shortens the drying time significantly, and hence reduces the energy consumption, but it also improves the appearance of the okara cake.

However, it is difficult to feed into the drying process with the conventional method, and drying is energy consuming and thus expensive. Therefore, it is more efficient to reduce the initial water content before drying. Mechanical compression is particularly well suited to eliminating water from high water content materials, as it uses 20 times less energy than thermal processes[15], however, it is difficult to apply the traditional mechanical compression dewatering technique to the fine residues from food processing. Therefore, some researchers have focused on the electro-osmotic dewatering (EOD) technique. In order to promote the efficiency of EOD and to depress some undesirable electrochemical reactions between the electrode and the material, these researchers have

used the AC electric field,[16,17,18,19] DR,[20,21] and a rotational electrode[22] at different electric field intensities for some material dewatering. However, this body of experimental work has almost exclusively used sludge[23,24,25,26,27] and some fine-grained sediment, such as quartz suspension,[22] kaolinite, bentonite,[22,29,30,31,32] and white clay.[17,28] The few food materials that have been investigated include okara,[16,20] tofu sheet,[21] and tomato paste suspension.[19]

During EOD, the Joule heat should be generated due to the current passing through the materials. However, only a few researchers mentioned the temperature increase during EOD.[24,25,28,32,33] Although some researchers reported the experimentally observed beneficial effects of EOD, the movement of water within the sample is not fully understood. The researchers mainly focused on the dewatering rate and the energy consumption, paying little attention to the effect of the EOD on the solids content of the drainage. The objectives of the present study are (1) to explore the temperature increase of okara, (2) to evaluate the energy efficiency ratio, and (3) to examine the effect of EOD on the solids content of the drainage.

Materials and Methods

Materials

Okara, with $79.9\%\pm0.21\%$ (wb) of the initial moisture content, was provided by Misuzu Co., Ltd., Japan. It was produced from cooked soybean mash. The zeta potential was $-1.99\,\mathrm{mV}$, measured with a potential meter (ZP-20, Shimadzu, Japan). It was stored in a refrigerator at 4℃ for a maximum of three days before use. Before sampling, some of the okara was removed from the refrigerator and laid in a testing room (20℃$\pm$1℃) for at least four hours.

Dewatering Setup

The setup (Fig. 1) was composed of a data logger system and an EOD system. The data logger system included a data logger (GR-3500, Keyence Japan), a current sensor (HCS-20-20-AP, URD Co., Japan), two electronic balances (GX-400, 0.001 g, A & D, Japan), and a T-type thermocouple (SUS316, Chino, Japan). The EOD system consisted of a function synthesizer (1915, NF Corpotation, Japan), a precision power amplifier (4510, NF Corporation, Japan), a frame, and an EOD cell. This cell was mainly composed of a dewatering tube (Plexiglas tube, 50 mm in inner diameter and 100
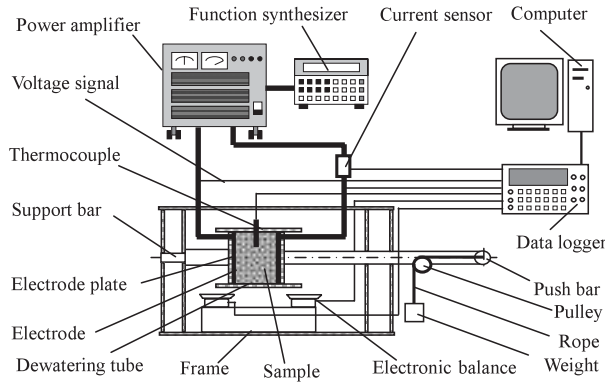
Fig. 1. Electro-osmotic dewatering setup

mm in length); two titanium sieve electrodes (14 mesh and covered with 100 mesh filter cloth); two Plexiglas plates with some channels for drainage, which were used to fix the electrodes (electrode plate); a support bar; and a push bar.

Methods and Procedure

The dewatering tube was carefully filled with the sample (50 g). The end face of the sample in the tube was lightly tapped with the right electrode plate in order to ensure that the electrode fully contacted the sample. The pressure applied to the sample was supplied by the right electrode plate, functioning as a piston moving towards the left, driven by an appropriate weight (14 kg) with a rope and a pulley.

In order to compare the effect of the electric field on the dewatering process, the experiments were performed twice: one series of okara sample was dewatered by mere pressure (pressure dewatering (PD)), and a parallel series was conducted at a constant pressure combined with an electric field (EOD). The moisture content of the sample and the solids content of the drainage were measured with an oven at 105℃.

After the sample was prepared and the system was connected (Fig. 1), the data logger system was started first; then pressure was gently applied to the sample. For the PD series, the test lasted 50 min with just pressure. For the EOD series, the sample was dewatered for 10 min by just pressure, then voltage was applied to the sample.

Evaluating the effect of the different electric fields on the dewatering involved the use of DC voltage (20 V, 30 V, and 40 V), AC voltage (square waveform, frequencies of 0.001 Hz, 0.002 Hz, and 0.01 Hz), and duty ratio (DR) voltage (DR of 90%, 80%, 70% and 60%), which is the ratio of the positive time to a cycle when the waveform is rectangular.

The effective value of the AC and the DR voltages was 20 V. When a DC voltage was applied, the electrode at the left end of the dewatering tube functioned as the cathode, and the electrode at the right end functioned as the anode. When DR voltage was introduced, the positive time of the right electrode plate functioning as the anode was longer than the negative time of the right electrode plate functioning as the cathode in one cycle. Therefore, the right electrode plate was regarded as the apparent anode, and the left electrode plate was denoted as the apparent cathode.

During dewatering, the voltage, the current, the mass of drainage discharged from both ends of the dewatering tube, and the temperature of the sample center were recorded at 10 s intervals and stored in a PC. In order to observe the curves clearly, 30 s was accepted as the time interval. Three replications were conducted for all samples under each experiment condition. Because the experiment results were not significantly different using a t-test at the 0.05 level, a single profile was reported.

The mass increment of the drainage discharged from the left electrode plate and the right electrode plate was calculated as:

$$\Delta m_{(L,R)} = m_{(L,R)\mathrm{E}t} - m_{(L,R)\mathrm{E}0} \qquad (1)$$

where $m_{\mathrm{E}0}$ is the accumulative mass of the drainage before the electric field treatment, g; $m_{\mathrm{E}t}$ is the accumulative mass of the drainage at time t under the electric field (including $m_{\mathrm{E}0}$), g. The subscript L denotes the left electrode plate, and R denotes the right electrode plate. When Eq. (1) was used to describe the mass increment of the drainage discharged from the left electrode plate, the subscript L was assigned, whereas the subscript R was assigned for that discharged from the right electrode plate.

Because the mass of the drainage removed with the electric field was more than that of the control in the same dewatering time, the excessive water resulting from the electric field application at a given time was denoted as the "EOD-water." The energy to evaporate the EOD-water at 100℃ was calculated as:

$$P = (m_{\mathrm{E}} - m_{\mathrm{P}}) \times 2256.3 \times 10^3 \qquad (2)$$

where m_{E} is the total mass of the drainage water dewatered during the EOD course, kg; m_{P} is the total mass of the drainage water dewatered during the PD course, kg; and 2256.3×10^3 is the latent heat of water at 100℃, J kg^{-1}.
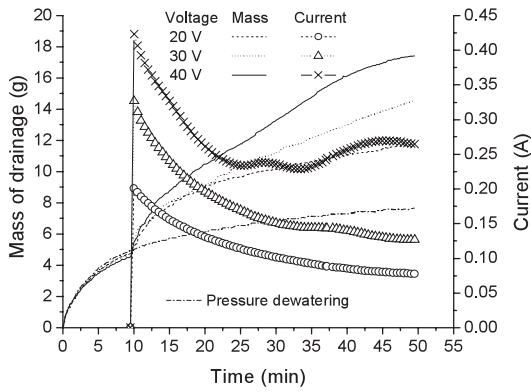
Fig. 2. Typical dewatering course of sample at 70kPa with different DC voltages
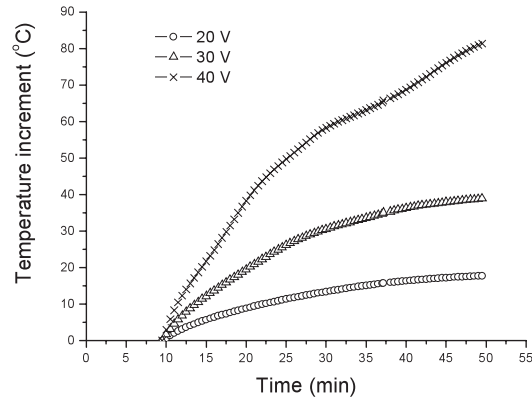

Fig. 3. Sample temperature increment during EOD

Li et al.[13] defined an energy efficiency ratio to evaluate the effect of the high-intensity electric field on promoting the drying rate of the okara cake drying with the electrohydrodynamic technique. In our research, the energy efficiency ratio was adopted for describing the effect of electro-osmosis on dewatering. It was defined as the ratio of the energy consumed for evaporating the water removed due to the electric field to the energy input to the electric field for EOD:

$$E_R = \frac{P}{P_e} \qquad (3)$$

where P is defined in Eq. (2); and P_e is the electric energy consumed by the electric field during EOD course, J. It can be calculated as

$$P_e = VIt \qquad (4)$$

where V is the effective value of the voltage applied to the sample, V; I is the effective value of the current passing through the sample, A; and t is the EOD time, s.

Results and Discussion

Effect of DC Voltage on Dewatering

Figure 2 depicts a typical PD course as well as an EOD course with different DC voltages at 70 kPa. The results indicated that more than 64% of the total drainage was removed after dewatering by pressure alone for 10 min, and then the mass of the drainage removed by pressure increased slowly. However, when an electric field was applied to the sample at the same pressure after 10 min for the PD course, the

drainage mass had a fast increment within a few minutes, and then increased gradually with an increase in time. The results also revealed that the dewatering rate increased with an increase in DC voltage. Saveyn et al.[34] observed this sudden increment phenomenon during EOD for activated sludge. They explained that it was caused by the electrolytic gas development and subsequent water displacement at the bottom electrode (cathode). The main setup used in their research was a vertical Plexiglass cylinder equipped with horizontal electrodes; the drainage discharged from the bottom electrode. However, Saveyn et al.[28] also performed an electro filtration of a quartz suspension with a two-sided electro filtration unit, which was a horizontal filter chamber. They indicated that the electrolytic gas produced at both electrodes was allowed to escape freely through the drainage tubes at both sides of the filter cake. The steep jump of the drainage mass did not result from the electrolytic gas. According to the theory of the electrical double layer and the principle of electro-osmosis, when the electric field is applied to the sample, some of the water absorbed on the surface of the colloid particles would be suddenly released, due to the effect of the external electric field.

Figure 2 plots the curves of the current vs. time for different voltages. It is known that the current increases with an increase in voltage. For 20 V and 30 V, the results indicated that the current quickly decreased in the initial stage and then decreased gradually with an increase in time, because the electrical contact resistance between the anode and the sample increased remarkably due to the water moving to the cathode during EOD.[28] However, when 40 V was applied to the sample, the current increased again with an increase in time

after a fast decrease that was probably caused by the Joule heat.

Figure 3 reveals that the sample temperature increment at different DC voltages increased with an increase in time. The rising temperature rate increased with an increase in voltage. These results differed from those reported by Yoshida,[18] Jumah et al.,[19] and Saveyn et al..[34] In an EOD test conducted with a type of kaolinite clay, Yoshida[18] suggested that the bubbles produced by electrolysis near the upper electrode were hardly visible, and there was hardly any temperature rise in the sludge bed caused by the Joule heat because of constant voltage (more than 40 V) conditions. Saveyn et al.[34] found that an electric field of 25 V m^{-1} was able to induce sufficient additional electro-osmotic water removal without major heat loss. Conducting an EOD using tomato paste at 2.5 V cm^{-1} with different wave forms and frequencies, Jumah et al.[19] determined that the amount of gases produced was not considerable, and observed no sludge temperature rise caused by Joule heating. However, the rise in temperature should not be ignored for okara dewatering with an electric field in this work.

Figure 4 (A) plots the curves of the mass of the drainage discharged from both ends of the dewatering tube vs. time. Both ends of the dewatering tube discharged drainage, and the mass of the drainage discharged from the left side (cathode) exceeded that discharged from the right side (anode). Moreover, the masses of the drainage discharged from both ends during the EOD course exceeded that during the PD course. This result differed from that reported by Saveyn et al..[28] In their electrofiltration experiment with a DC electric field, the filtrate volume discharged from the anode was less than that without the electric field. The reason for this difference can be explained as follows. Both electrodes in their research were fixed; however, in this work the right electrode plate simultaneously functioned as a piston that moved towards the left side after pressure was applied to it. When the right electrode plate moved toward the left, it should drive the drainage to flow within the sample toward the left, but some of the drainage was discharged from the right side. This phenomenon occurred for two reasons: first, the right electrode was also a sieve; second, there was friction at the liquid-solid boundaries in the microchannel of the sample. During dewatering, the drainage was so great that it could not flow quickly from the left side through the microchannels, espe-
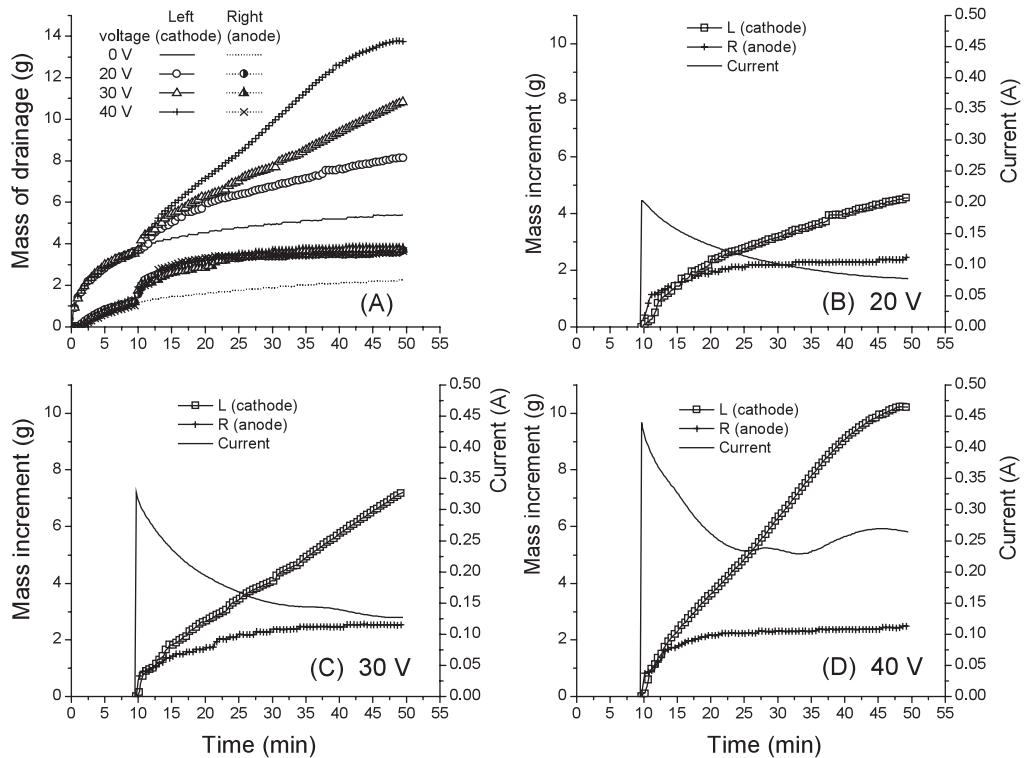

Fig. 4. Drainage mass and mass increment as well as current change with time

cially in the initial period after pressure was applied. Therefore, some of the drainage was discharged from the anode.

Figure 4 (A) also illustrates that drainage mass suddenly and simultaneously increased at both sides when a DC electric field was applied to the sample. Although the steep jump of drainage mainly took place at the anode side, the drainage discharge from the cathode was dominant during EOD. The fast increase in the mass of the drainage continued for 5 min. After that, the mass increment of the drainage discharged at the anode side increased slowly, and its flux was almost equal to the mass flux of the drainage dewatered by pressure alone. Therefore, we concluded that the DC voltage did not significantly affect the mass flux of the drainage discharged from the anode. However, the mass increment of the drainage discharged from the cathode increased rapidly with increasing time, and the mass flux of the drainage at a high voltage exceeded that at a low voltage.

Figures 4 (B), (C), and (D) reveal that the mass increment of the left drainage and the right drainage, as well as the current, changed with time at different voltages. It is important to mention that the mass increment Δm_R was larger than the mass increment Δm_L in the initial period (3 min) after an electric field was applied to the sample. The difference between the mass increment (Δm_R-Δm_L) at the right (anode) end and that at the left (cathode) end of the dewatering tube was more remarkable at 20 V. This finding initially seemed illogical because the zeta potential of okara was -1.99 mV, meaning that the capillary matrix within the sample was negatively charged. According to electro-osmotic theory, the

water should move from the anode to the cathode (i.e. from the right side to the left side) along the dewatering tube under the experiment conditions. Thus, the mass increment Δm_L should have been larger than Δm_R. However, the results were reversed (Fig. 4). The reason for this phenomenon was as previously explained. The okara cake is considered a porous material. With a large amount of water filling the pores within it, some of the water is absorbed by the cellulose and protein.[13] The water contained in okara is difficult to remove by mechanical pressure because of its compressibility and colloidality; it should be mainly bound water. When a DC electric field was applied to the sample, some of the bound water was suddenly released from the surface of the colloid particles. Water released from the surface of the colloid particles flowed to the cathode plate driven by the electric field. However, some of the water, especially that near the anode plate, could not easily move toward the cathode through the microchannel because of the flow friction and the fact that the dewatering tube was fixed horizontally. As a result, the momentary mass increment of the drainage flowing out from the right electrode (anode) was greater than that flowing out from the left electrode plate (cathode).

According to the principle of electrophoresis and electro-osmosis, the electric field applied to the sample should resist the protein and the fiber particles moving to the cathode. Figure 5 presents the effect of the DC voltage on the solids content of the drainage. Fig. 5 (A) demonstrates that the solids content of the drainage discharged at the anode was significantly less than that at the cathode when more than 20 V was applied to the sample under the experiment condi-
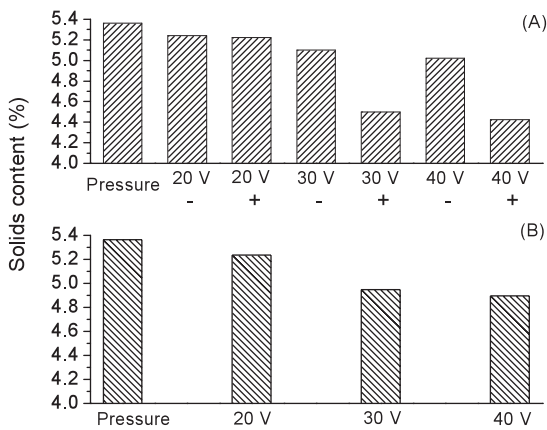

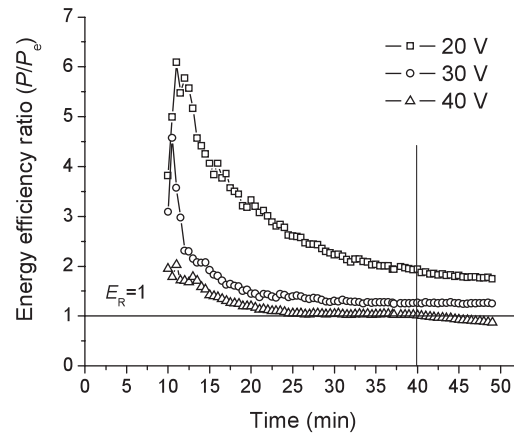Fig. 5. Effect of DC voltage on drainage solids content

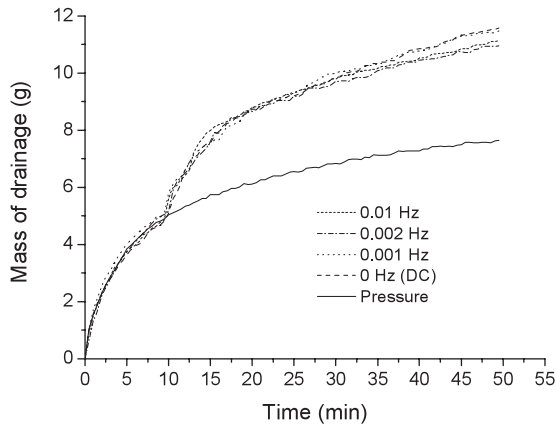Fig. 6. Effect of voltage on energy efficiency ratio

Fig. 7. Effect of frequency on drainage mass at different frequencies

Fig.8. Temperature increment change with time at different frequencies

tions.

The weight average solids content of the drainage changed with voltage (Fig. 5 (B)). The results indicated that the solids content of the drainage removed during the EOD course was lower than that removed during the PD course, and that the solids content of the drainage decreased with the increase in voltage applied to the sample. We concluded that more nutritional components remained in okara after dewatering with electro-osmosis. This result is very important for reusing okara.

The energy efficiency ratio at different voltages changed with time (Fig. 6). In the initial period (less than 1 min), the energy efficiency ratio quickly rose when a lower voltage was applied to the sample and then decreased quickly with increasing time. The results also indicated that the energy efficiency ratio decreased with increasing voltage, as a result of Joule heat losses. Figure 6 indicates that the energy efficiency ratio was the highest at 20 V and always exceeded one during the experiment. However, when the voltage was 40 V, the energy efficiency ratio was lower than one after 30 min, as a result of additional Joule heat loss. Therefore, the voltage applied to the sample should be 20 V under the experiment conditions, in view of energy efficiency.

Although the Joule heat losses resulted in a decrease in the energy efficiency ratio during EOD, the temperature rise had the positive effects of pasteurization and deactivation of some antinutritional factors, especially trysin inhibitor.

Effect of AC Voltage on Dewatering

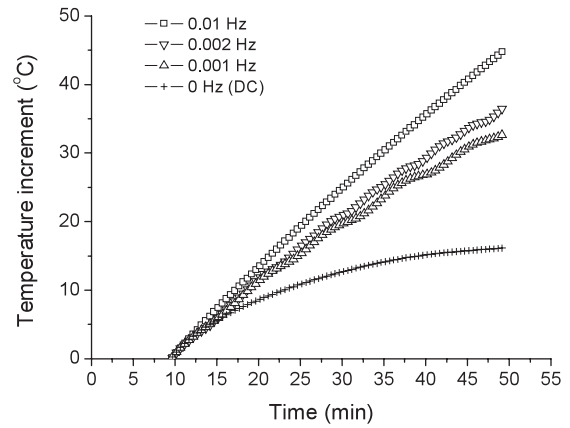Figure 7 plots the curves of the drainage mass vs. time dur-

ing the PD and EOD courses with AC voltage at different frequencies (20 V, RMS). When an AC voltage was applied to the sample, the relationship between the drainage mass and the time was almost the same as that with a DC voltage. Therefore, the drainage mass was not significantly influenced by different frequencies under the experiment conditions. This result did not agree with the results reported by Yoshida et al.,[17] Li et al.,[20] and Jumah et al..[19] Their results indicated that frequency had a positive effect on the dewatering rate. The disparity between our results and theirs may be due to the differences in the physical and chemical properties of the materials, procedures, electric field intensities, and other undetermined factors. Therefore, further work is still needed.

The temperature increased with an increase in frequency (Fig. 8), indicating that more Joule heat was generated due to high frequency. For 0.01 Hz, the temperature increment increased almost linearly with time.

Yukawa et al.[35] developed the following equation to describe the kinetics of liquid removal in pressurized EOD of a saturated porous material in order to explain the behavior of the interstitial liquid in saturated water media under dewatering with pressure aided by an electric field.

$$q = q_p + q_E = -\frac{1}{\mu\alpha\rho_s(1-\varepsilon)}\frac{\partial P_L}{\partial z} - \frac{D\varphi(\varepsilon)\zeta}{k\mu}\frac{\partial \psi}{\partial z} \qquad (5)$$

were, q is the superficial liquid velocity, m s^{-1}; α is the specific cake resistance, m kg^{-1}; ρ_s is the density of solid particles, kg m^{-3}; μ is the liquid viscosity, Pa s; z is the coordinate, m; P_L is the liquid pressure in cake pores, Pa; k is a particle shape factor, (-); D is the dielectric constant of the inter-

stitial liquid, F m^{-1}; ζ is the particle zeta potential, V; ψ is the electric potential; and V. $\phi(\varepsilon)$ is a function of the cake porosity ε(-) dependent on the material being dewatered. The first term in Eq. (5) represents the Darcy law proportionality between the liquid velocity and the pressure gradient, which mainly depends on the specific cake resistance α, the cake porosity ε, and the liquid viscosity μ. The electro-osmotic contribution is described by the second term, which is a function of liquid electro kinetic parameters (zeta potential), electric field parameters, and the cake structure parameters ε. When voltage was applied to the sample with the setup used in this work, if the right electrode plate was the anode and the moving direction of the water within the sample driven by the electro-osmosis was the same as that driven by the pressure, the water would move from the right electrode plate towards the left electrode plate; in this case, the mass of the drainage should increase due to the decrease in viscosity. If the right electrode was the cathode, the flow driven by electro-osmosis moved from the left side to the right side; the effects of pressure and electro-osmosis were opposite, according to Eq. (5). Determining the effect of the sample temperature on the drainage was complicated. Although the temperature of the sample increased with the increase in frequency and decreased with the increase in the DR of the voltage, the frequency and the DR (discussed later) of the voltage did not significantly affect the drainage mass. From Eq. (5), the electric potential gradient, the pressure gradient, the porosity, and the zeta-potential, in addition to the drainage viscosity, influence the drainage behavior. Although the force (the electric potential gradient and the pressure gradient) for moving the drainage within the sample increased due to the decrease of the electrode gap during EOD, the porosity of the sample and the modulus of the zeta potential of the sample decreased.

Figure 9 plots the curves of the current as well as the mass increment of the drainage vs. time at different frequencies of AC voltage. The results indirectly confirmed that the effective value of the current increased with increasing time. The current tended to increase with increasing frequency. At a higher frequency (0.01 Hz), the instantaneous modulus of the current decreased with time when the polarity of the electrode did not change. However, the instantaneous modulus of the current increased at first and then decreased with time within the half cycle, except during the first half cycle, when the frequency was lower (0.002 Hz and 0.001 Hz). In order to explain the current increase with increasing frequency under

AC electric field conditions, Yoshida et al.[17] introduced an electrical equivalent circuit, consisting of a resistance and a capacitance in parallel. With EOD, the moisture content of the sample, especially the portion near the anode, decreased quickly; the dielectric constant of the sample should increase gradually, increasing the sample capacitance and resistance, and the capacitance should store a greater charge. The current would increase during this period. As the capacitance charged, the current would decrease due to the increase in the sample resistance if the polarity of the electrode did not change. After the polarity of the electric field reversed, the capacitance should discharge and then charge again. Therefore, the capacitance alternately charged and discharged with the change in the electric field polarity.
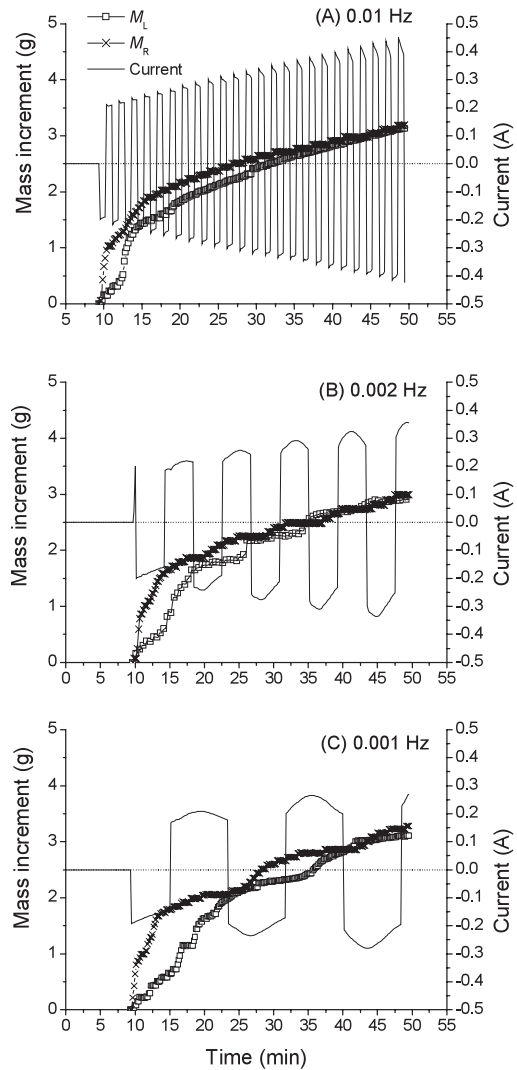

Fig. 9. Drainage mass increment as well as current change with time and frequencies
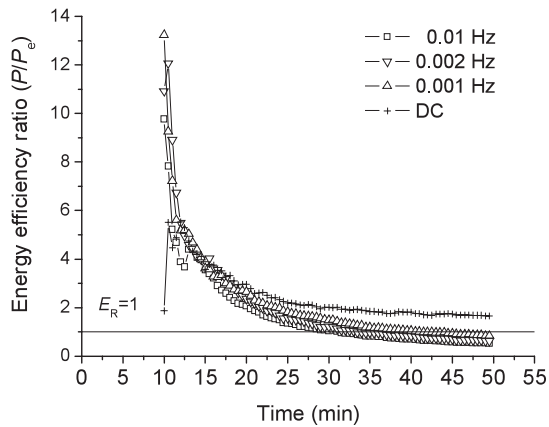
Fig. 10. Effect of frequencies on energy efficiency ratio

Table 1. Effect of frequency on drainage solids content

Frequency (Hz)	0.01	0.002	0.001	DC
Solids content (%)	5.16	4.90	4.89	5.08

When an AC square waveform voltage was applied to the sample during EOD, the two electrodes functioned as anode or cathode for equal times within one cycle; therefore, the mass of the drainage discharged from the two electrodes should be the same. The results (Fig. 9) agreed well with this prediction under the experiment conditions. When the frequency of the AC electric field was lower (0.001 Hz and 0.002 Hz), the alternating fast increment of the drainage mass discharged from the two electrode plates was clearly observed in Figs. 9 (B) and (C). The results also confirmed that the direction of the water movement within the okara along the microchannel changed with the polarity of the electric field. Figures 9 (A), (B), and (C) also indicate that the mass increment Δm_R was larger than the mass increment Δm_L in the initial period after an AC electric field was applied to the sample. However, in these cases, the main reason was that the right electrode first functioned as the anode when an AC voltage was applied to the sample.

The energy efficiency ratio changed with time at different frequencies (Fig. 10). This tendency was similar to that with the DC voltage. However, the energy efficiency ratio with AC voltage was higher than that with DC voltage in the initial period of the EOD course. Furthermore, the energy efficiency ratio decreased quickly with time, especially when a higher frequency voltage was applied to the sample, due to Joule heat losses.

The solids content of the drainage increased with increasing frequency (Table 1). Therefore, a lower frequency electric field should be applied to the sample during EOD to maintain the solids content in okara and achieve a high energy efficiency ratio.

Effect of DR Voltage on Dewatering

Under the different DRs at 0.002 Hz, the changes in the drainage mass and temperature increment with time tended to be similar to those for the AC voltages. The average final mass (11.69 g $\pm$ 0.18 g) of the drainage removed with the different DRs slightly exceeded that (10.95 g) removed with AC voltage at 0.002 Hz. However, the DR did not significantly affect the drainage mass. The final temperature increments at the different DRs were 18.66℃ at 90%, 20.32℃ at 80%, 26.19℃ at 70%, and 33.19℃ at 60%. The temperature increased with decreasing DR, increasing quickly when the lower DR voltage was applied to the sample. Therefore, it can be concluded that more Joule heat losses occurred when the lower DR voltage was applied to the sample.

Figure 11 plots the curves of the drainage mass increment as well as the current vs. time for the different DRs. The mass increments of the drainage discharged from the left electrode plate (apparent cathode) significantly exceeded that discharged from the right electrode plate (apparent anode), however, when 60% of the DR electric field was applied to the sample during EOD, the mass increments of the drainage discharged from both electrode plates were same. Figures 11 (B), (C) and (D) imply that the effective current decreased with increasing time within the positive half cycle, except for the first perfect positive half cycle. However, the effective current increased with increasing time during the negative half cycle except for the first negative half cycle, indicating that the total electrical resistance of the sample should decrease with increasing time in the negative half cycle for the following reason. The moisture content of the sample near the piston (the right electrode plate) was lower than that of the sample near the dead end (the left electrode plate) in the PD course. When the sample was exposed to a DR electric field at a constant mechanical pressure, the distribution of the water in the sample would change due to electro-osmosis. During the positive half cycle, the moisture content of the sample near the right electrode decreased quickly. The com-
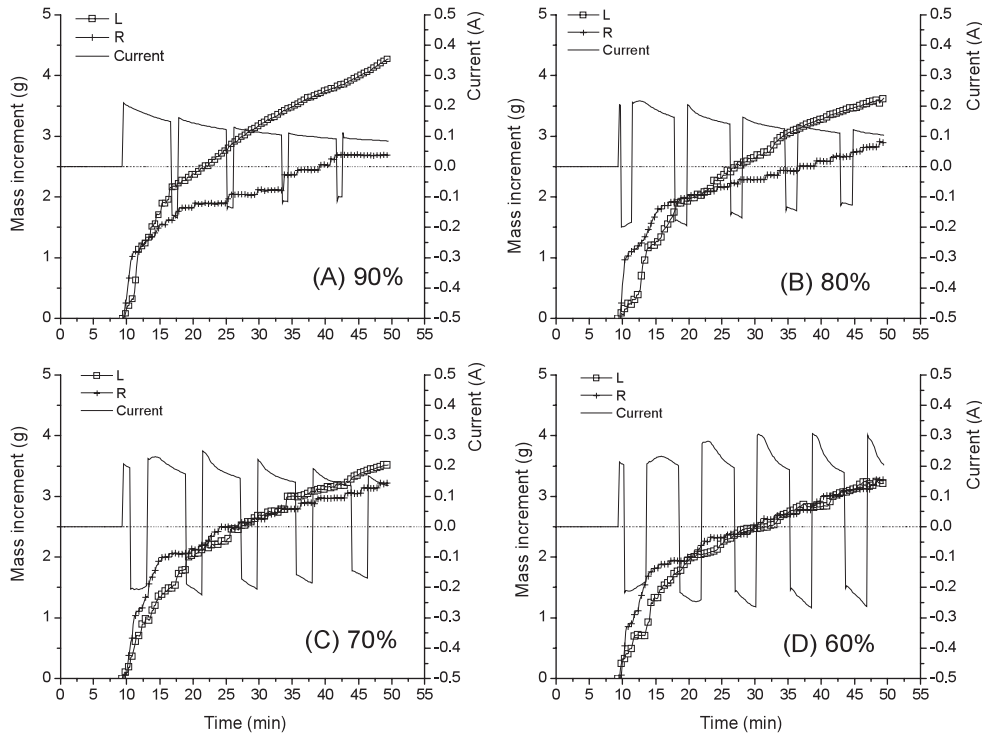
Fig. 11. Drainage mass increment as well as current change with time and DR at 0.002 Hz

Table 2. Effect of duty ratio on drainage solids content

Duty ratio (%)	90	80	70	60
Solids content (%)	5.00	4.98	4.98	5.06

Fig. 12. Effect of DR on energy efficiency ratio at different duty ratios

bination of pressure and the electro-osmosis increased the contact resistance between the sample and the right electrode, resulting in a decrease in the effective current. In contrast, during the negative half cycle, some of the water would move to the piston, causing the moisture content of the portion sample near the right electrode plate to increase and the contact resistance to decrease because the effect of electro-osmosis on water movement within the sample was opposite that of the pressure. Therefore, the effective current gradually increased with time during the negative half cycles.

Figure 12 plots the energy efficiency ratio change with time at the different DR voltages. The change in the energy efficiency ratio with time at different DRs was similar to that at different frequencies; however, the energy efficiency ratio decreased with decreasing DR of the voltage. Therefore, a higher DR should be used in practice from an energy-conser-
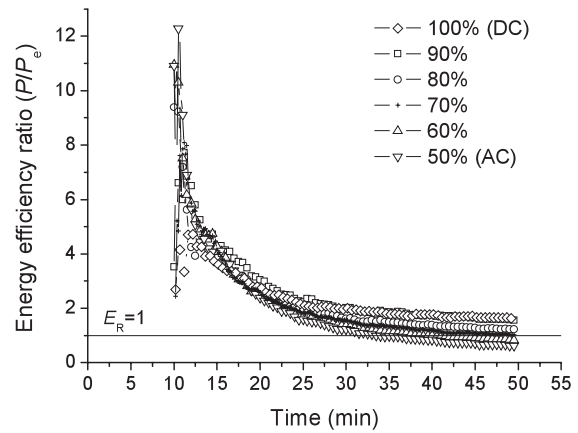
vation point of view.

The solids content of the drainage at different DR voltages and 0.002 Hz is listed in Table 2. The results indicate that the DR did not significantly affect the solids content of the drainage.

Acknowledgements

References

1) Wei, X., Current situation and development trend of tofu industry in China-a review. *Soybean and Technology*, **485**, 10-11. in Japanese, (2006).

2) Khare, S. K., Jha, K., and Gandhi, A. P., Citric acid production from okara (soy-residue) by solid-state fermentation. *Bioresource Technology*, **54**, 323-325, (1995).

3) Taruna, I., and Jindal, V. K., Drying of soy pulp (okara) in a bed of inert particles. *Drying Technology*, **20**, 1035-1051, (2002).

4) O'Toole, D. K., Characteristics and use of okara, the soybean residue from soy milk productions-a review. *Journal of Agricultural and Food Chemistry*, **47**(2), 363-371, (1999).

5) Chan, W.-M., and Ma, C.-Y., Acid modification of proteins from soymilk residue (okara). *Food Research International*, **32**, 119-127 (1999).

6) Suntornsuk, W., Pochanavanich, P., and Suntornsuk, L., Fungal chitosan production on food processing by-products. *Process Biochemistry*, **37**, 727-729, (2002).

7) Hsieh, C., and Yang, F.-C., Reusing soy residue for the solid-state fermentation of *Ganoderma lucidum*. *Bioresource Technology*, **91**(1), 105-109 (2004).

8) Heck, J. X., Hertz, P. F., and Ayub, M. A. Z., Extraction optimization of xylanases obtained by solid-state cultivation of *Bacillus circulans* BL53. *Process Biochemistry,* **40**, 2891-2895 (2005).

9) Quitain, A. T., Oro, K., Katoh, S., and Moriyoshi. T., Recovery of oil components of okara by ethanol-modified supercritical carbon dioxide extraction. *Bioresource Technology*, **97**(13), 1509-1514, (2006).

10) Isobe, S., Production technology of biodegradable materials using agricultural wastes. *Farming Japan*, **37**(5), 21-25, 33 (2003).

11) Isobe, S., Development of water proof biodegradation materials with agricultural by-products such as tofu residue, okara. *Soybean and Technology*, **485**, 18-23. in Japanese (2006).

12) Wachiraphansakul, S., and Devahastin, S., Drying kinetics and quality of soy residue (okara) dried in a jet spouted bed dryer. *Drying Technology*, **23**, 1229-1242, (2005).

13) Li, F.-D., Li, L.-T., Sun, J.-F., and Tatsumi, E., Electrohydrodynamic (EHD) drying characteristic of okara cake. *Drying Technology*, **23**, 565-580, (2005).

14) Li, F.-D., Li, L.-T., Sun, J.-F., and Tatsumi, E., Effect of electrohydrodynamic (EHD) technique on drying process and appearance of okara cake. *Journal of Food Engineering*, **77**, 275-280, (2006).

15) Leclerc, D., and Rebouillat, S., Dewatering by Compression. In A. Rushton (Eds), *Mathematical models and design methods in solid-liquid separation* (pp: 356-391). The Netherlands: Martinus Nijhoff Publishers, (1985).

16) Isobe, S., Uemura, K., and Noguchi, A., Dewatering of soybean residue "okara" by electro-osmosis and screw press. In Alex Buchanan (Eds.), *Proceedings of the Second International Soybean Processing and* Utilization *Conference* (pp. 523-527). Bangkok, Thailand: Funny Publishing Limited Partnership (1996).

17) Yoshida, H., Kitajyo, K., and Nakayama, M., Electroosmotic dewatering under A. C. electric field with periodic reversals of electrode polarity. *Drying Technology*, **17**(3), 539-554, (1999).

18) Yoshida, H., Electro-osmotic dewatering under intermittent power application by rectification of A.C. electric Field. *Journal of Chemical Engineering of Japan*, **33**(1), 134-140, (2000).

19) Jumah, R., Al-Asheh, S., Banat, F., and Al-Zoubi, K., Electroosmotic dewatering of tomato paste suspension under AC electric field. *Drying Technology*, **23**(7), 1465-1475, (2005).

20) Li, L., Li, X., Uemura, K., and Tatsumi, E., Electroosmotic dewatering of okara in different electric fields. In *Proceedings of 99 International Conference on Agricultural Engineering* (pp. IV58-IV63). Beijing, China, (1999).

21) Xia, B., Sun, D.-W., Li, L.-T., Li, X.-Q., and Tatsumi, E., Effect of electro-osmotic dewatering on the quality of tofu sheet. *Drying Technology*, **21**(1), 129-145, (2003).

22) Ho, M. Y., and Chen, G., Enhanced electro-osmotic dewatering of fine particle suspension using a rotating anode. Industrial & *Engineering Chemistry Research,* **40**(8), 1859-1863 (2001).

23) van Diemen, A. J. G., de Vet, M. J. H., and Stein, H. N., Influence of surfactants on electra-osmotic dewatering of sludges. *Colloids and Surfaces*, **35**, 57-64, (1989).

24) Laursen, S., and Jensen, B. J., Electroosmosis in filter cakes of activated sludge. *Water research*, **27**(5), 777-783, (1993).

25) Zhou, J., Liu, Z., She, P., and Ding, F., Water removal from sludge in a horizontal electric field. *Drying Technology*, **19**(3&4), 627-638, (2001).

26) Raats, M. H. M., van Diemen, A.J.G. Lavèn, J. and Stein, H.N., Full scale electrokinetic dewatering of waste sludge. *Colloids and Surfaces A: Physicochemical and Engineering Aspects*, **210** (2 & 3), 231-241, (2002).

27) Saveyn, H., Curvers, D., Pel, L., de Bondt, P., and Van der Meeren, P., In situ determination of solidosity profiles during activated sludge electrodewatering. *Water Research*, **40**, 2135-2142, (2006).

28) Saveyn, H., Van der Meeren, P., Hofmann, R., and Stahl, W., Modelling two-sided electrofiltration of quartz suspensions: Importance of electrochemical reactions. *Chemical Engineering Science*, **60**, 6768 - 6779, (2005).

29) Iwata, M., Igami, H., Murase, T., and Yoshida, H., Analysis of electroosmotic dewatering. *Journal of Chemical Engineering of Japan*, **24**(1), 45-50, (1991a).

30) Iwata, M., Igami, H., Murase, T., and Yoshida, H., Combined operation of electroosmotic dewatering and mechanical expression. *Journal of Chemical Engineering of Japan*, **24**(3), 399-401, (1991b).

31) Iwata, M., Sato, M., Nagase, H. 2004. Analysis of creep deformation in electro-osmotic dewatering. *Asian Pacific Confederation of Chemical Engineering Congress progress Program and Abstract*, 232-241.

32) Larue, O., Wakeman, R.J., Tarleton, E.S., and Vorobiev, E., Pressure electroosmotic dewatering with continuous removal of electrolysis products. *Chemical Engineering Science*, **61**, 4732-4740, (2006).

33) Larue, O., Mouroko-Mitoulou, T., and Vorobiev, E., Pressurized electroosmotic dewatering in a filter cycle. *Drying* Technology, **19**(9), 2363-2377, (2001).

34) Saveyn, H., Pauwels, G., Timmerman, R., and Van der Meeren, P., Effect of polyelectrolyte conditioning on the enhanced dewatering of activated sludge by application of an electric field during the expression phase. *Water Research*, **39**, 3012-3020, (2005).

35) Yukawa, H., Chigira, H., Hoshino, T., and Iwata, M., Fundamental study of electroosmotic filtration. *Journal of Chemical Engineering of Japan*, **4**, 370-376, (1971).

オカラの電気浸透脱水での温度上昇、エネルギー効率、固形率に及ぼす電界条件の影響

李法徳・李修渠・五月女格・五十部誠一郎

山東農業大学，食品総合研究所，UNU-KIRIN フェロー

日本で毎年多く発生する豆腐・豆乳製造時の副産物であるオカラについては，その有効利用のための効率的脱水技術の開発が求められている．筆者らは，今まで，電気浸透処理を用いたオカラの脱水処理について検討を加えてきた．ここでは，電気浸透処理時の電界条件がオカラの脱水時の温度上昇やエネルギー効率，固形率に及ぼす影響について報告する．実験は，水平に設置した電気浸透脱水処理装置で実施した．電極は，チタニウム製のメッシュタイプを用いて，加圧条件は70kPaとした．電界条件としては，直流，交流（矩形波），さらに通電率を制御したもの（矩形波：以下DR処理）を用いて有効電圧は20Vとした．

この電界条件では，オカラの脱水時の温度上昇は無視できるレベルであった．またオカラ内部の水分変化は，両面の電極に向けて脱水が進行し，特に処理初期においてこの傾向は顕著であった．直流では，電圧の上昇に伴って脱水率が進行したが，交流，DR処理では，あまり電圧の影響は認められなかった．エネルギー効率（電気浸透処理のために投入したエネルギーに対して電気浸透効果による脱水量の蒸発に必要なエネルギーの比により算出）は，初期において大きく1を上回ったが，処理時間の経過によって急激に低下して，最終的には1以下となった．脱液部の固形分については，直流処理では電圧増加によって減少し，交流処理では，周波数の増加に応じて増加したが，DR処理では条件による変化はほとんどなかった．これらのオカラの脱水処理に関する電気浸透法での基礎諸言は，同様に高水分系の食品副産物の再資源化のための効率的な脱水操作として有益な情報である．